[11] R. J. King, "Electromagnetic wave propagation over a constant impedance plane," *Radio Sci.*, vol. 4, pp. 255–268, 1969.
[12] J. R. Wait, "On the wave tilt at high frequencies—A personal view," *IEEE Trans. Electromagn. Compat.*, vol. 39, p. 65, Feb. 1997.
[13] V. Cooray, "Predicting the spatial and temporal variation of the electromagnetic fields, currents, and speeds of subsequent return strokes," *IEEE Trans. Electromagn. Compat.*, vol. 40, pp. 427–435, Nov. 1998.
[14] ——, "On the concepts used in return stroke models applied in engineering practice," in *Proc. Int. Conf. Electromagnetics in Advanced Applications (ICEAA)*, 1999, pp. 771–776.
[15] R. Thottappill, V. A. Rakov, and M. A. Uman, "Distribution of charge along the lightning channel: Relation to remote electric and magnetic fields and to return stroke models," *J. Geophys. Res.*, vol. 102, pp. 6987–7006, 1997.
[16] C. A. Nucci, G. Deindorfer, M. A. Uman, F. Rachidi, M. Ianoz, and C. Mazzetti, "Lightning return stroke current model with specified channel base current: A review and comparison," *J. Geophys. Res.*, vol. 95, pp. 20 395–20 408, 1990.
[17] M. A. Uman and D. K. McLain, "Magnetic field of lightning return stroke," *J. Geophys. Res.*, vol. 74, pp. 6899–6910, 1969.

On the Modeling of a Gapped Power-Bus Structure Using a Hybrid FEM/MoM Approach

Yun Ji and Todd H. Hubing

***Abstract*—A hybrid finite-element-method/method-of-moments (FEM/MoM) approach is applied to the analysis of a gapped power-bus structure on a printed circuit board. FEM is used to model the details of the structure. MoM is used to provide a radiation boundary condition to terminate the FEM mesh. Numerical results exhibit significant errors when the FEM/MoM boundary is chosen to coincide with the physical boundary of the board. These errors are due to the inability of hybrid elements on the boundary to enforce the correct boundary condition at a gap edge in a strong sense. A much better alternative is to extend the MoM boundary above the surface of the board.**

***Index Terms*—Finite element boundary element (FE-BE), finite element method of moments (FE-MoM), hybrid FEM/MoM, power-bus structures.**

I. Introduction

The hybrid finite-element method/method-of moments (FEM/MoM) also abbreviated as FE-MM, and which is also referred to as finite element boundary element (FE-BE), finite element boundary integral (FE-BI), or finite element boundary element (FEM/BEM) in the literature, is an electromagnetic modeling technique that is well suited for analyzing printed circuit board (PCB) structures [1]–[3]. With this method, an electromagnetic problem is first divided into interior and exterior equivalent problems. The interior equivalent problem is modeled using FEM. The exterior equivalent problem is represented by a surface integral equation, e.g., the electric-, magnetic- or combined-field integral equation (EFIE, MFIE, or CFIE) and solved using the MoM. FEM and MoM problems are related by enforcing the continuity of the tangential fields on the boundary. The coupled FEM and MoM equations provide a unique and exact solution to Maxwell's equations in both the interior and exterior regions.

Manuscript received March 12, 2002; revised July 2, 2002.

Y. Ji is with the Desktop Architecture Lab, Intel Corporation, Hillsboro, OR 97124 USA.

T. H. Hubing is with the Dept.of Electrical and Computer Eng., University of Missouri-Rolla, Rolla, MO 65401 USA.

Digital Object Identifier 10.1109/TEMC.2002.804775

Gapped power-bus structures are widely used to distribute power on high-speed digital PCBs [4]–[6]. In this study, a hybrid FEM/MoM approach is used to analyze a gapped power-bus structure. The accuracy of the solution depends on the location of the FEM/MoM boundary.

II. Hybrid FEM/MoM

The FEM approach used in this work is based on the weak form of the vector wave equation [2]

$$\int_V \left[\left(\frac{\nabla \times \mathbf{E}(\mathbf{r})}{j\omega\mu_0\mu_r} \right) \bullet (\nabla \times \mathbf{T}(\mathbf{r})) + j\omega\varepsilon_0\varepsilon_r \mathbf{E}(\mathbf{r}) \bullet \mathbf{T}(\mathbf{r}) \right] dV = \int_S (\hat{n} \times \mathbf{H}(\mathbf{r})) \bullet \mathbf{T}(\mathbf{r}) dS - \int_V \mathbf{J}^{\text{int}}(\mathbf{r}) \bullet \mathbf{T}(\mathbf{r}) dV \quad (1)$$

where S is the surface enclosing volume V; $\mathbf{T}(\mathbf{r})$ is the weighting (testing) function, and $\mathbf{J}^{\text{int}}$ is an impressed source. The electric field is approximated using the vector tetrahedral elements proposed by Barton and Cendes [9]. The tangential magnetic field is expanded using the triangular patch elements proposed in [10]. A Galerkin method is used to discretize (1) as follows:

$$\begin{bmatrix} A_{ii} & A_{is} \\ A_{si} & A_{ss} \end{bmatrix} \begin{bmatrix} E_i \\ E_s \end{bmatrix} = \begin{bmatrix} 0 & 0 \\ 0 & B_{ss} \end{bmatrix} \begin{bmatrix} 0 \\ J_s \end{bmatrix} + \begin{bmatrix} g_i \\ g_s \end{bmatrix} \quad (2)$$

where A_{ii}, A_{is}, A_{si}, A_{ss}, and B_{ss} are sparse coefficient matrices; and g_i and g_s are source terms.

The FEM volume is bounded by MoM surface elements. MoM is used to solve an EFIE of the following form [11, ch. 6] as shown in (3) at the bottom of the next page. The equivalent electric current $\mathbf{J}(\mathbf{r})$, and magnetic current $\mathbf{M}(\mathbf{r})$ are expanded using the same triangular patch elements that are employed by the FEM portion of the code.

After discretizing the EFIE, the MoM matrix equation is in the following form:

$$[C][J_s] = [D][E_s] - \left[F^i\right] \quad (4)$$

where $[C]$ and $[D]$ are coefficient matrices, and $[F^i]$ is the excitation term. If the geometry contains a perfect electric conductor (PEC), the PEC boundary condition $\hat{n} \times \mathbf{E} = 0$ is enforced, which effectively eliminates these elements and reduces the number of unknowns.

Equations (2) and (4) form a coupled and determined system. There are three different solution methods that can be used to solve the coupled matrix equation [7], [12]. The *outward-looking* solution method is employed in this study. The preconditioning technique reported in [12] is used to improve the convergence rate and accuracy of the iterative solvers. Procedures used to model the source and load and to calculate scattering parameters are provided in [13].

III. Numerical Results and Analysis

Gapped power-bus structures are used in digital PCB designs to supply different voltage levels to devices of different logic families while sharing a common return plane. Gaps are also used to control the flow of low-frequency currents on a plane and thereby prevent "noisy" devices from interfering with nearby components that are sensitive to power-bus noise [4], [5].

Fig. 1 shows the geometry of a simple gapped power-bus structure. The board is 152.4 × 101.6 × 2.4 mm. The bottom plane (the ground plane) is copper and modeled as a PEC surface. The top plane (the power plane) is also copper except that there is a 5.1-mm wide gap located at the center along the z-axis. The material between the top and bottom planes has a dielectric constant that varies with frequency. The

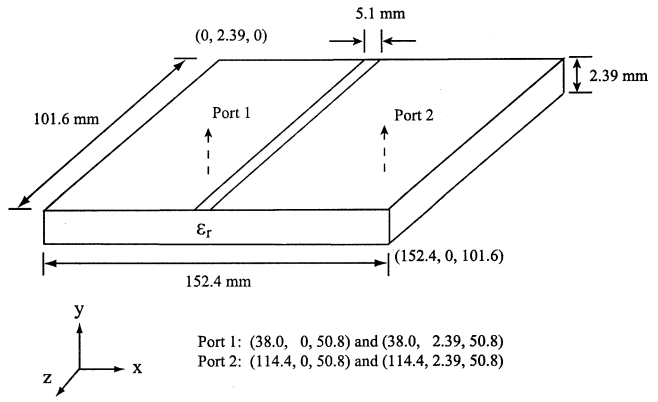

Fig. 1. Geometry of a gapped power-bus structure.

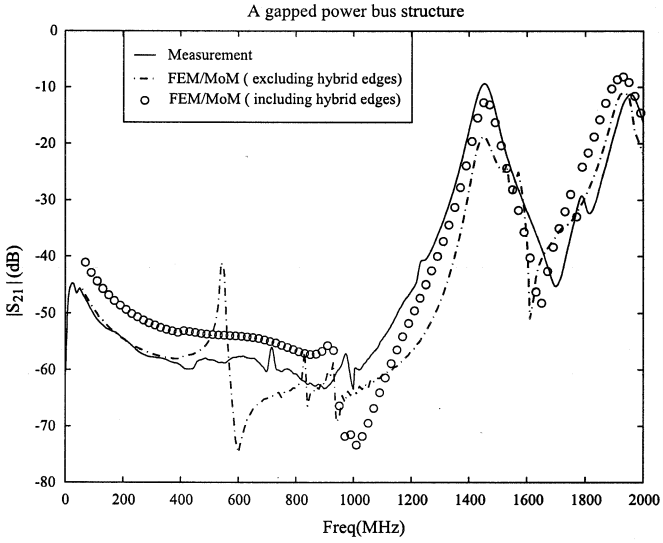

Fig. 2. Measured and numerical $|S_{21}|$ results for the gapped power-bus structure.

dielectric constant and loss tangent were determined using an experimental approach [14]. An approximate value for the dielectric constant as a function of frequency is given by

$$\varepsilon_r \approx \begin{cases} 4.6(1-j0.01) & \text{Frequency} < 400\ \text{MHz} \\ 4.4(1-j0.015) & 400\ \text{MHz} > \text{Frequency} < 1.0\ \text{GHz} \\ 4.2(1-j0.02) & 1.0\ \text{GHz} > \text{Frequency} < 2.0\ \text{GHz} \end{cases}.$$

An experimental board was built and two standard connector designator (SMA) connectors were attached to the port locations designated in Fig. 1. A 50-Ω network analyzer was used to measure the magnitude of the transfer coefficient, $|S_{21}|$. The measured results are plotted in Fig. 2.

There is no dc connection between the two ports. Therefore, little power is coupled from Port 1 to Port 2 at low frequencies. However, the coupling between the two ports is strong at frequencies corresponding to certain board resonances. The first $|S_{21}|$ peak appears at 1.45 GHz, which corresponds to the TM^y_{02} cavity mode of each power patch. The

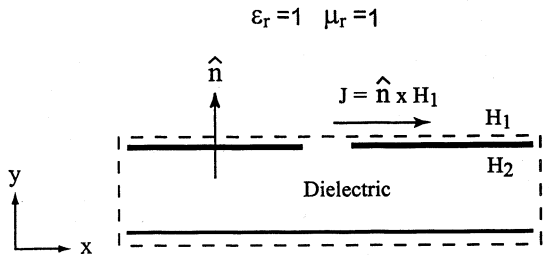

Fig. 3. MoM boundary coincides with the physical boundary of the board.

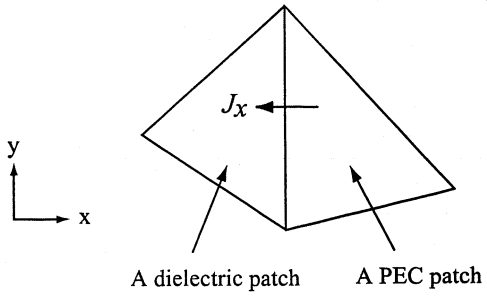

Fig. 4. Hybrid edge links a dielectric patch and a PEC patch.

TM^y_{01} mode at 720 MHz is not excited because the two ports are located at the center of each power patch along the z-axis. The second $|S_{21}|$ peak at 1.95 GHz corresponds to the TM^y_{20} mode of each power patch. The TM^y_{10} mode at 970 MHz and the TM^y_{11} mode at 1.79 GHz are not efficiently excited because the two ports are located near the center of each power patch along the x axis.

The hybrid FEM/MoM code presented in [2], employing the formulation described in the previous section, is used to model this geometry. The MoM boundary surface can be chosen arbitrarily as long as the exterior equivalent problem is homogenous and the scalar Green's function can be used to construct the EFIE. In this study, two different boundaries are chosen that lead to numerical results with different accuracy.

A. Case 1: MoM Boundary Coincides With the Board Surface

The MoM boundary is commonly chosen to coincide with the physical boundary of the board as shown in Fig. 3. This is a convenient choice for two reasons. First, locating the boundary on a PEC surface yields a smaller number of unknowns for the equivalent magnetic current because the tangential E-field is forced to zero. Second, the equivalent electric current $\mathbf{J}$ on the PEC surface, which is given by $\hat{n} \times \mathbf{H}$, is then equal to the current on the outside of the PEC surface.

The MoM boundary shown in Fig. 3 includes both dielectric and PEC surfaces. Fig. 4 shows part of the mesh on the dielectric-PEC interface. An edge linking one dielectric surface patch and one PEC surface patch is referred to as a *hybrid edge* in this paper. An important consideration is how the boundary conditions on hybrid edges are enforced.

Insight to the physics near hybrid edges can be obtained from analytical solutions for conducting wedge problems. Fig. 5 shows a thin two-dimensional (2-D) conducting wedge. A theoretical analysis shows that

$$\frac{\mathbf{E}(\mathbf{r})}{2} = \mathbf{E}^{\text{inc}}(\mathbf{r}) + \int_S \left[\begin{array}{c} -\mathbf{M}(\mathbf{r}') \times \nabla' G_0(\mathbf{r}, \mathbf{r}') - jk_0\eta_0 \mathbf{J}(\mathbf{r}') G_0(\mathbf{r}, \mathbf{r}') \\ +j\frac{\eta_0}{k_0} \nabla' \bullet \mathbf{J}(\mathbf{r}') \nabla' G_0(\mathbf{r}, \mathbf{r}') \end{array} \right] dS' \tag{3}$$

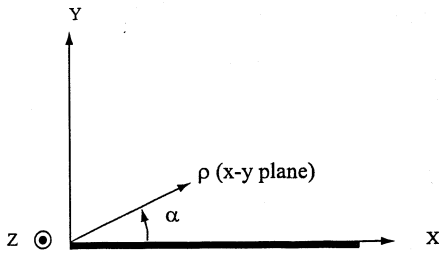

Fig. 5. A 2-D thin perfect conducting wedge.

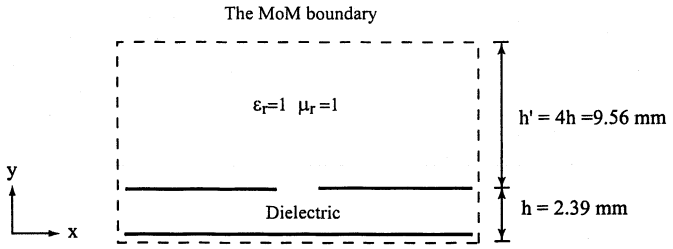

Fig. 6. MoM boundary is raised above the gapped plane.

the z components of the electric and magnetic fields (E_z and H_z) near the edge (wedge end) are given by [11, ch. 4], [5]

$$E_z \propto \rho^{0.5} \tag{5}$$

$$H_z \propto b + \rho^{0.5} \tag{6}$$

where ρ is the distance from the field point to the edge and b is a constant determined by the problem itself. Therefore, the equivalent magnetic and electric currents across a hybrid edge, designated as M_x and J_x in Fig. 4, are given by

$$M_x = E_z \times \hat{y} = 0 \text{ as } \rho \to 0 \tag{7}$$

$$J_x = \hat{y} \times H_z = b \text{ as } \rho \to 0. \tag{8}$$

No unknowns for the magnetic current need to be assigned to hybrid edges, since the value of this current approaches zero. However, (8) indicates that the equivalent electric current on one side of the PEC surface is not zero. Therefore, unknowns for the equivalent electric current must be assigned to hybrid edges. It is worth noting that the actual (physical) current across a hybrid edge, which is given by $\hat{n} \times (\mathbf{H}_1 - \mathbf{H}_2)$ as shown in Fig. 3, is zero because the unit normals for the top and bottom surfaces are opposite [15]. When modeling PEC surfaces with a nonhybrid MoM technique, the equivalent electric current is generally equal to the actual current. Therefore, MoM techniques that model the total current on PEC surfaces generally exclude hybrid edges in numerical simulations. This effectively forces the current to zero across these edges.

In the hybrid FEM/MoM, excluding the hybrid edges can lead to erroneous results. As shown in Fig. 2, the FEM/MoM results exhibit a false resonance near 550 MHz when the hybrid edges are excluded. The results above 1 GHz are also significantly different from the measurement. When the hybrid edges are included in MoM calculation, the false resonance around 550 MHz is eliminated and the accuracy of the numerical results is improved near the first resonance at 1.45 GHz. However, there are still significant errors under 1.2 GHz. The likely reason for this error is that the fringing fields near the gap are the dominant contributor to the coupling between the two ports. Linear tetrahedral and triangular patch elements do not model the fringing fields very well. Numerical experiments show that the errors can be partially reduced by using a very fine MoM mesh in the region near the gap. However, fine-mesh densities dramatically increase the computer resources required to solve the problem.

B. Case 2: The MoM Boundary Extends Above the Board Surface

Another approach to the solution of this problem is illustrated in Fig. 6. The MoM boundary is chosen to coincide with the board's bottom plane and extends 9.56 mm above the gap. A relatively fine tetrahedral FEM mesh is used in the gap region and gradually transitions to a coarse mesh on the MoM boundary. By raising the MoM boundary above the gap, the total number of MoM unknowns can be kept small despite the fine mesh in the vicinity of the gap. MoM has a memory requirement of $O(N^2)$, while FEM is $O(N)$. Therefore, this mesh strategy can reduce the amount of memory required for the hybrid FEM/MoM solution. Table I compares the computer memory required to model Case 1 and Case 2. The FEM region in Fig. 6 is much larger than that in Fig. 3. However, the additional computer memory required by the FEM is more than compensated for by the reduction in computer memory required by the MoM. Fig. 7 plots the measured and modeled $|S_{21}|$ results. The numerical results agree with the measurement fairly well.

TABLE I
COMPARISON BETWEEN CASE 1 AND CASE 2

	Number of FEM unknowns	Number of MoM unknowns	Computer memory requirement (Mbytes)
Case 1	1,452	2,451	176
Case 2	4,521	2,217	158

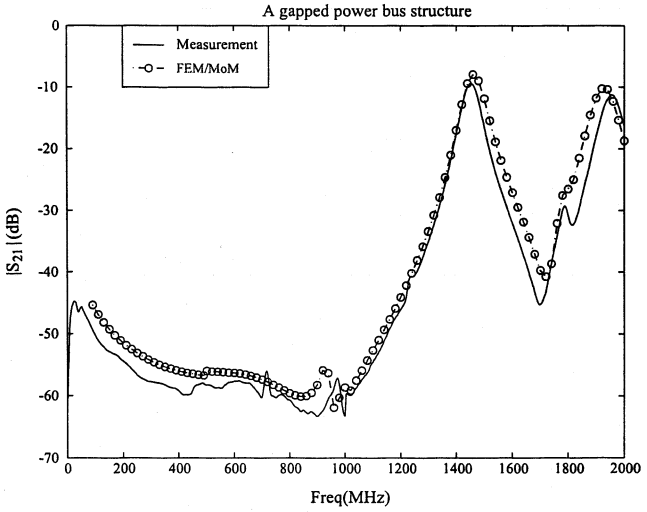

Fig. 7. $|S_{21}|$ for the gapped power-bus structure with the MoM boundary raised above the surface of the board.

IV. SUMMARY

Two approaches to modeling gapped power-bus structures on PCBs using a hybrid FEM/MoM method have been presented. For this problem, it is important to model the fringing electric fields near the gap. When the FEM/MoM boundary is chosen to coincide with the physical boundary of the board, the equivalent electric current cannot be forced to zero on the hybrid edges even though the actual electric current is zero across these edges. Therefore, it is important to have a relatively fine mesh near the gap in order to adequately model the fringing fields.

Problems associated with having the gap on the boundary can be avoided by raising the FEM/MoM boundary above the gap, effectively increasing the size of the FEM region. Then, small tetrahedral elements can be used around the gap and a coarse triangular mesh can be used on the MoM boundary. Computational resources are reduced using this approach because the increased memory requirements to model the FEM region are more than offset by the reduction in memory required to model the MoM surface. Numerical results obtained using this approach agree well with measurements.

REFERENCES

[1] T. F. Eibert and V. Hansen, "3-D FEM/BEM-hybrid modeling of surface mounted devices within planar circuits," *IEEE Trans. Microwave Theory Tech.*, vol. 46, pp. 1334–1336, Sept. 1998.

[2] Y. Ji and T. H. Hubing, "EMAP5: A 3D hybrid FEM/MoM code," *Appl. Computat. Electromagn. Soc. (ACES) J.*, vol. 15, pp. 1–12, 2000.

[3] H. Wang, Y. Ji, T. H. Hubing, and J. L. Drewniak, "Radiation from right angle bends in microstrip traces," in *Proc. IEEE Int. Symp. Electromag. Compat.*, Washington, DC, Aug. 2000.

[4] "Pentium III Processor Power Distribution Guidelines," Intel Corp., Intel App. Note AP-907, order 245 085-001, 1999.

[5] Z. Soe, "Layout Guideline for the RC7100 Motherboard System Clock," Fairchild Semiconductor Corporation, Fairchild Semiconductor App. Bull. AB-19, stock no. AB00 000 019, 1998.

[6] J. Chen *et al.*, "Power-bus isolation using power islands in printed circuit boards," *IEEE Trans. Electromagn. Compat.*, vol. 44, pp. 373–380, May 2002.

[7] A. F. Peterson, S. L. Ray, and R. Mittra, *Computational Methods for Electromagnetics*. New York: IEEE Press, 1997, ch. 11.

[8] M. L. Barton and Z. J. Cendes, "New vector finite elements for three-dimensional magnetic field computation," *J. Appl. Phys.*, vol. 61, pp. 3919–3921, 1987.

[9] J. L. Volakis, A. Chatterjee, and L. C. Kempel, *Finite Element Method for Electromagnetics*. New York: IEEE Press, 1998, pp. 56–59.

[10] S. M. Rao, D. R. Wilton, and A. W. Glisson, "Electromagnetic scattering by surfaces of arbitrary shape," *IEEE Trans. Antennas Propagat.*, vol. AP-30, pp. 409–418, May 1982.

[11] J. J. H. Wang, *Generalized Moment Methods in Electromagnetics*. New York: Wiley, 1990.

[12] Y. Ji, H. Wang, and T. H. Hubing, "A novel preconditioning technique and comparison of three formulations for the hybrid FEM/MoM method," *Appl. Computat. Electromagn. Soc. (ACES) J.*, vol. 15, pp. 103–114, 2000.

[13] Y. Ji and T. H. Hubing, "On the interior resonance problem when applying a hybrid FEM/MoM approach to model printed circuit boards," *IEEE Trans. Electromag. Compat.*, vol. 44, pp. 318–323, May 2002.

[14] C. Wang, "Determining Dielectric Constant and Loss Tangent in FR-4," Electromagnetic Compatibility Lab., Dep. Elect. Comput. Eng., University of Missouri-Rolla, Rolla, MO, TR00-1-41.

[15] J. Van Bladel, *Singular Electromagnetic Fields and Sources*. New York: Oxford Univ. Press, 1991, ch. 4.

Finite-Element Modeling of Coaxial Cable Feeds and Vias in Power-Bus Structures

Hao Wang, Yun Ji, and Todd H. Hubing

***Abstract*—This paper presents three different models that can be used to represent coaxial cable feeds or vias in printed circuit board power-bus structures. The *probe model* represents a coaxial feed or via as a current filament with unknown radius. The *coaxial-cable model* enforces an analytical field distribution at the cable opening or via clearance hole. The *strip model* employs the equivalent radius concept to represent cylindrical feeds and vias as rectangular strips. Although the strip model is functionally equivalent to two closely positioned probe models, it accurately represents the conductor radius and is more accurate in situations where the via or feed radius is important.**

***Index Terms*—Circuit board modeling, edge elements, finite-element method (FEM), method of moments (MOM).**

I. INTRODUCTION

Multilayer printed circuit boards (PCBs) and multichip modules (MCMs) often employ a power-bus structure consisting of solid power-return plane pairs. At low frequencies, the behavior of the power-bus structure can be modeled using lumped elements [1]. At frequencies where the dimensions of the board are not electrically small, it is necessary to use complex distributed models. In the frequency domain, two numerical methods often used to analyze PCB structures are the method of moments (MoM) and the finite-element method (FEM).

It is critical to accurately represent sources and vias when modeling the behavior of PCB power-bus structures. When making measurements, these structures are often driven with a coaxial cable. The outer conductor of the coaxial cable is connected to the reference plane and the center conductor extends through to the power plane. The reference plane is normally calibrated to the cable opening, where the center conductor begins to extend beyond the outer conductor. The term via commonly refers to a plated-thru hole in a PCB. A via can be used for mounting a through-hole component or for routing signals between layers. The geometry of vias and coaxial feeds is similar. Both consist of an opening in one or both planes and a vertical conductor that may or may not connect to each plane.

This paper investigates three models that can be used to represent sources and vias in a PCB power bus. The *probe model* represents coaxial cable feeds and vias using one finite-element or moment-method-element edge. The *coaxial-cable model* enforces the analytical field distribution at the opening in the reference plane and includes the effects of the finite radius of the vertical conductor. The *strip model* employs the equivalent radius concept [2] to replace cylindrical feeds or vias with rectangular strips. These three models have been implemented in a hybrid FEM/MoM code. Two practical power-bus structures are investigated to validate and compare the three models.

Manuscript received March 15, 2002; revised June 19, 2002.

H. Wang and T. H. Hubing are with the Department of Electrical and Computer Engineering, University of Missouri-Rolla, Rolla, MO 65409 USA.

Y. Ji is with the Desktop Architecture Laboratory, Intel Corporation, Hillsboro, OR 97124 USA

Digital Object Identifier 10.1109/TEMC.2002.804776